Asian Journal of Chemistry; Vol. 34, No. 9 (2022), 2435-2443

ASIAN JOURNAL OF CHEMISTRY

https://doi.org/10.14233/ajchem.2022.23848

Kinetic and Thermodynamic Studies of Ion Exchange Process in Removal of Ca^{2+} and Mg^{2+} from Cooling Tower Water using Amberlite IR 120 and Amberjet 1200

ROBERT MBEDZI*, HILARY RUTTO and TUMISANG SEODIGENG

Clean Technology and Applied Materials Research Group, Department of Chemical and Metallurgical Engineering, Vaal University of Technology, Private Bag X021, South Africa

*Corresponding author: E-mail: robertm@vut.ac.za

Received: 23 March 2022; *Accepted*: 28 July 2022; *Published online*: 19 August 2022; AJC-20944

In this study, the thermodynamics and kinetics parameters of the ion exchange process in removing Ca^{2+} and Mg^{2+} from cooling tower water using Amberlite IR1200 and Amberjet were investigated. Thermodynamics and kinetics were studied by varying the amount of contact time (min), adsorbent (mL), temperature (K), concentration (mg/L) and pH of the solutions. The effectiveness of pecentage removal was found to rely on pH, as there was a significant increase of removal percentage Ca^{2+} and Mg^{2+} from pH of 3 to 6. The contact time was reached after 60 min on both resins. The correlation coefficients (R^2) of Langmuir, Freundlich and Tempkin isotherms ranged from 0.92 to 1, suggesting that the experimental data best described the models. However, correlation coefficients (R^2) for the D-R model range between 0.5 to 0.8, which means that experimental data does not fit the model well. Thermodynamic functions such as entropy (ΔS^o), enthalpy (ΔH^o) and change of free energy (ΔG^o) were obtained from the gradient and intercepts of straight-line graphs. The positive values of ΔG^o indicated that the adsorption is not spontaneous. Positive values of ΔH^o were found, meaning the endothermic type of adsorption, which indicates the chances of physical adsorption. The correlation coefficient (R^2) values of pseudo-first-order, pseudo-second-order and intraparticle models ranged from 0.89 to 1 on both metals. This observation indicates that pseudo-first-order, pseudo-second-order and intraparticle diffusion models best describe the experimental data in removing Ca^{2+} and Mg^{2+} from cooling tower water.

Keywords: Amberlite IR120, Amberjet 1200, Ca^{2+}, Mg^{2+}, Thermodynamics, Kinetics and isotherms.

INTRODUCTION

Heavy metals residuals have become a challenging issue worldwide on cooling towers and cooling water blow-down in all industrial manufacturers and utilities. Ca^{2+} and Mg^{2+} ions are the significant concerns released due to metals in the feed water and corrosion in the cooling tower system. The recirculating cooling water systems remove waste heat from environment. The power plant cooling system consists of the towers, circulation water pumps, pipelines and heat exchanger network. In cooling towers, heat is removed through evaporation and dissolved constituents of the recirculating water become concentrated. To excessive concentrations of certain constituents, part of the recirculating water is removed as blow-down. Therefore, make-up water must be added to the circulating water system to maintain an acceptable water salinity and conductivity [1]. Most industrial production processes rely on cooling tower water for efficient and proper operations. Industries such as refineries, food plants, manufacturing plants, petrochemical plants, steel mills, electric utilities and chemical processing plants depend on cooling water systems to perform duties daily [2]. Three of the main problems of cooling water systems are corrosion, scaling and biofouling depending on raw water conditions, pre-treatment, chemical treatment and concentration cycle [2]. Raw water used in the recirculating system is usually provided from rivers and underground. The underground water is harder and contains more alkalinity and total dissolved solids than the river.

Several methods have been studied to remove Ca^{2+} and Mg^{2+} from cooling tower water, such as electrodialysis [3-5], reverse osmosis [5,6], adsorption [6-10], electrocoagulation and ion exchange [10]. Among these methods, the ion exchange process seems to be effective in reducing concentrations of heavy metals because it is environmentally friendly, economically viable, selective and produces less sludge volume [10]. Several studies on the removal of heavy metals by ion exchange have been studied [10-12] and reported that the ion exchange

method could overcome problems encountered in other techniques.

The study focused on the thermodynamics and kinetics of ion exchange process in removing Ca^{2+} and Mg^{2+} from the cooling tower by using Amberjet 1200 and Amberlite IR 120. The effect of contact time (min), pH, temperature (K), concentration (mg/L) and amount of resins (mL) were investigated. The experimental data was described by Langmuir, Freundlich, Tempkin and Dubinin-Radushkevich (D-R) isotherms. The rate-controlling mechanisms for the ion exchange process were investigated by testing the experimental data with Lagergren's pseudo-first-order, pseudo-second-order kinetics and intraparticle diffusion. The ion exchange spontaneity of Ca^{2+} and Mg^{2+} on aqueous solutions using thermodynamic models were also determined.

EXPERIMENTAL

Amberjet 1200 and Amberlite IR 120 strong cation ion exchange resins in hydrogen form were obtained in Dow Chemicals Company, South Africa. The properties of the resins are given in Table-1. The resins were washed three times with a solution of 1 HCl and NaOH to remove possible organic and inorganic solutions trapped in the resins during the preparation. The resins were then washed several times with distilled water to convert Na^+ form to H^+ form by flushing the ion exchange column with 1 HCl and used out through the experiment.

Solution preparations and reagents: The solutions of Ca^{2+} and Mg^{2+} were prepared by dissolving an analytical grade $CaCl_2{\cdot}2H_2O$, $MgCl_2{\cdot}6H_2O$ (Merck, South Africa), respectively. Deionized and purified water was prepared by a Milli-Q water purification system and used throughout the experiment.

The percentage of Ca^{2+} and Mg^{2+} removal from aqueous solution by Amberjet 1200 and Amberlite IR 120 resins was calculated according to eqn. 1:

$$\text{Removal (\%)} = \frac{C_i - C_f}{C_f} \times 100 \quad (1)$$

where C_i and C_f are the initial and final concentrations (mg/L), respectively.

Column experiments: Column experiments were performed using a glass tube of 3 cm diameter and 30 cm height. The schematic diagram of the experimental setup is shown in Fig. 1. The experiments were conducted using one factor at a time method and the following parameters were varied throughout the experiment, concentration of Ca^{2+} and Mg^{2+} mg/L (200 to 600), pH (2-6) resins dosage mL (25 to 100) and contact time (20 to 90 min). All the experiments were carried out at a room temperature of 25 ºC. The Ca^{2+} and Mg^{2+} solutions having an initial concentration of 600 mg/L and 300 mg/L were prepared and used throughout the experiment. A peristaltic pump fed the Ca^{2+} and Mg^{2+} solutions on the ion exchange column. The treated solutions were collected from the exit at the time intervals and measured for the remaining Ca^{2+} and Mg^{2+}. The concentrations of Ca^{2+} and Mg^{2+} solutions were determined by atomic absorption spectrometer (AAS) and the pH was measured with a glass electrode.

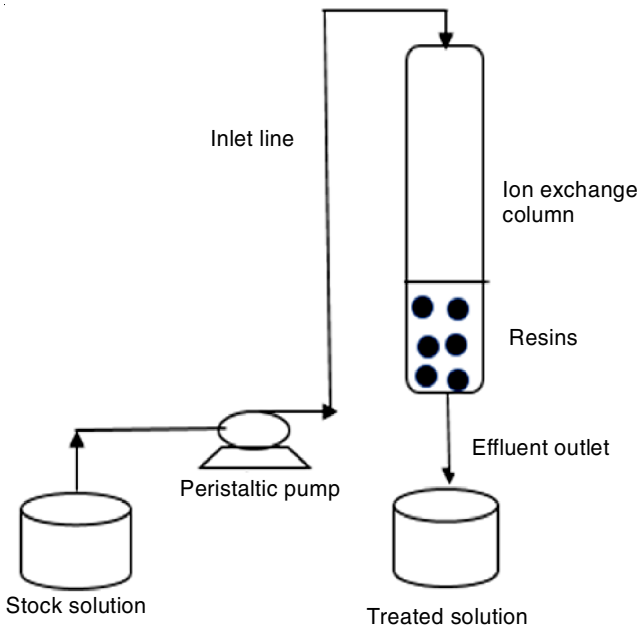

Fig. 1. Experimental setup for ion exchange column

TABLE-1
PROPERTIES OF AMBERJET 1200 AND AMBERLITE IR 1200 RESINS

Parameter	Amberjet 1200 (Na^+ form)	Amberlite IR 120 (Na^+ form)
Physical form	Amber spherical beads	Amber spherical beads
Matrix	Styrene divinylbenzene copolymer	Styrene divinylbenzene copolymer
Functional group	Sulfonate	Sulfonate
Ionic form as shipped	Na^+	Na^+
Total exchange capacity	≥ 2.00 eq/L (Na^+ form)	≥ 2.00 eq/L (Na^+ form)
Moisture holding capacity	43% to 47% (Na^+ form)	45% to 50% (Na^+ form)
Shipping weight	850 g/L	840 g/L
Service flow rate	5 to 50 BV/h	5 to 40 BV/h
Regeneration		
Regenerant	NaCI HCI H_2SO_4	NaCl HCl H_2SO_4
Level (g/L)	40 to 240 40 to 150 20 to 200	80 to 250 50 to 150 60 to 240
Concentration (%)	10 4 to 10 1 to 8	10 5 to 8 0,7 to 6
Minimum contact time	20 min	30 min
Slow rinse	2 BV at regeneration flow rate	2 BV at regeneration flow rate
Fast rinse	1 to 3 BV at a service flow rate	2 to 4 BV at a service flow rate

*1 BV (bed volume) = 1 m^3 solution per m^3 resin

RESULTS AND DISCUSSION

Effect of contact time: The effect of contact time on the removal of Ca^{2+} and Mg^{2+} using Amberlite IR120 and Amberjet 1200 is shown in Fig. 2a-b by varying times from 15 to 120 min. It is well known that the rate of adsorption plays a vital role in industries. When contact time increases, the % removal of Ca^{2+} and Mg^{2+} increased until it has reached an equilibrium point at about 60 min on both resins. The increase in % removal of Ca^{2+} and Mg^{2+} was due to the availability of exchangeable sites on the surface of the resins [13]. The highest % removal of Ca^{2+} was 98.3% for Amberlite IR120 and 87% for Amberjet 1200 as shown in Fig. 2a. Whereas, % removal of Mg^{2+} was 98% for Amberlite IR120 and 86.77% for Amberjet 1200. There was no significant increase in % removal of Ca^{2+} and Mg^{2+} when the process reached equilibrium; however, there was a % removal slightly decrease observed immediately after the equilibrium stage. As the available sites are reduced, the % removal of heavy metals decreases because of the increase in the repulsive forces between the alkaline metal ions and those in the liquid phase [14]. As a result, an equilibrium time of 60 min was used for the rest of the experiments.

Effect of dosage: Fig. 3a-d shows the effect of Amberlite IR1200 and Amberjet 1200 dosage in removing Ca^{2+} and Mg^{2+}

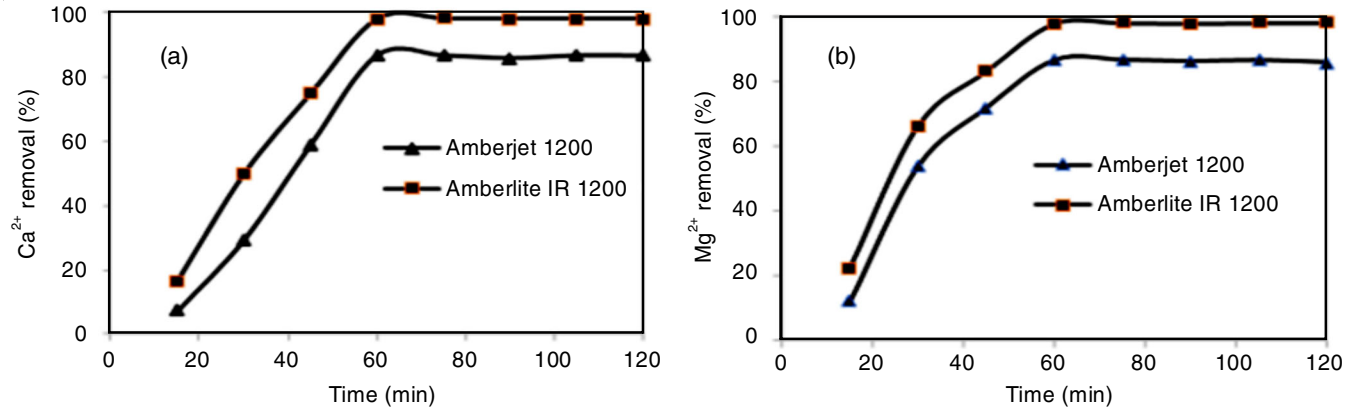

Fig. 2. Effect of contact time on the removal of Ca^{2+} (a) and Mg^{2+} (b) using Amberlite IR1200 and Amberjet 1200 (Ca^{2+} = 600 ppm, Mg^{2+} = 300 ppm, dosage = 15 mL, pH = 3 and Temp. = 25 °C)

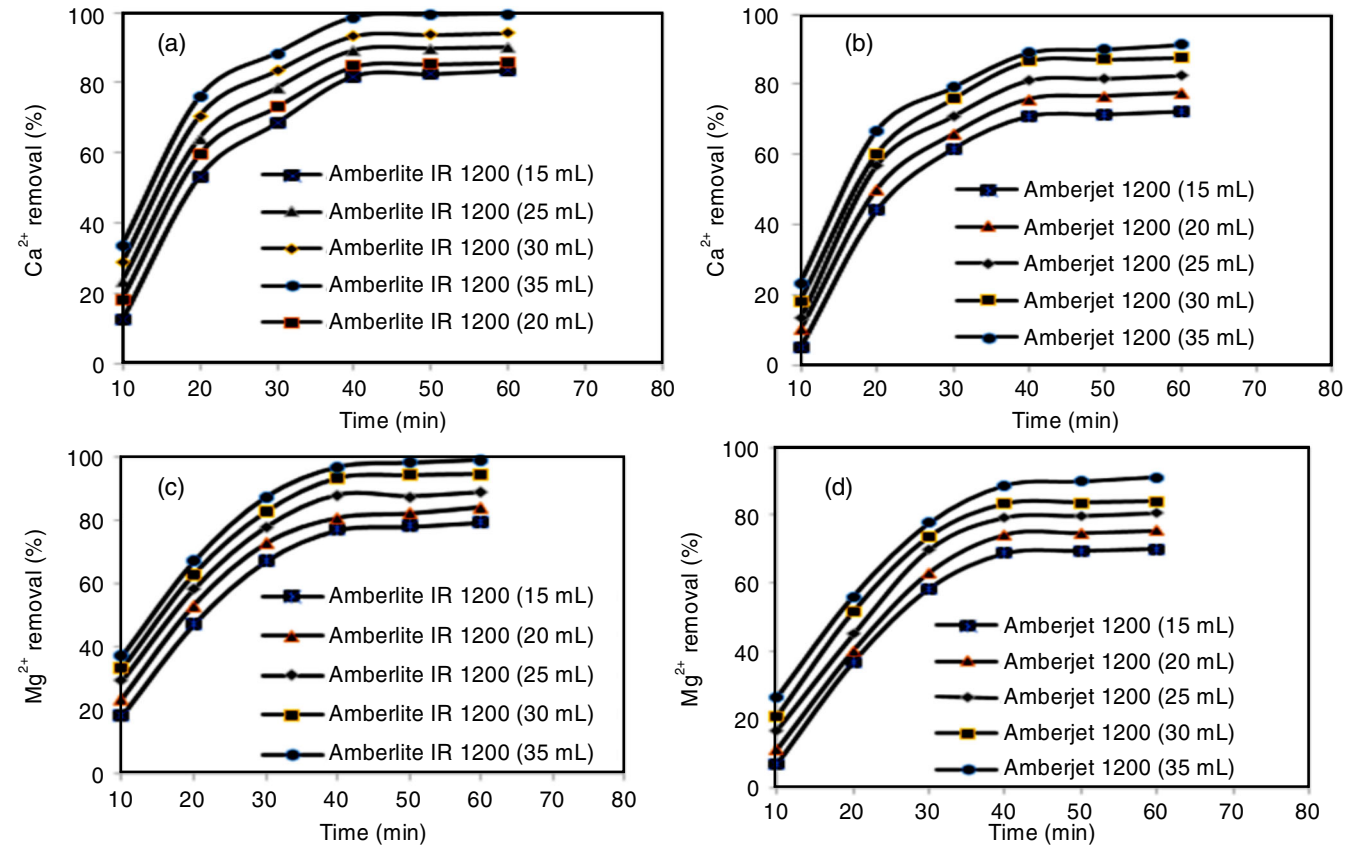

Fig. 3. Effect of dosage on the removal of Ca^{2+} and Mg^{2+} using Amberlite IR1200 (a and c) and Amberjet 1200 (b and d) (Ca^{2+} = 600 ppm, Mg^{2+} = 300 ppm, contact time = 60 min, pH = 3 and Temp. = 25 °C)

from cooling tower water by varying dosage from 15 mL to 35 mL while other parameters were kept constant. The highest % removal of Ca^{2+} was found to be 99.59% using Amberlite IR120 and 91.33% using Amberjet 1200 at the resin's dosage of 35 mL. Another highest % removal of Mg^{2+} was found to be 99.33% using Amberlite IR120 and 91.17% using Amberjet 1200 at the resins dosage of 35 mL. This is a result of availability of binding sites on the surface of the adsorbent [15]. This suggests that the maximum adsorption is achieved after a specific dose of the resins and this led to the constant % increase of heavy metals with further addition of the resins.

Effect of concentration: Fig. 4a-d show the effect of concentration in removing Ca^{2+} and Mg^{2+} studied by varying concentration from 100 to 300 ppm for Mg^{2+} and from 400 to 800 ppm for Ca^{2+}. The graphs show that the highest % removal of Ca^{2+} was observed from 22.45 to 99.078 using Amberlite IR1200 and 16.25 to 89% using Amberjet 1200 at 100 mg/L. The graphs also show the highest % removal of Mg^{2+} from 20 to 99.35% using Amberlite IR1200 and 15 to 91 using Amberjet at 100 mg/L. However, adsorption % removal decreased with an increase in the initial metal ion concentration. Heavy metals in the aqueous solution interact more with the binding sites at lower concentrations than in higher concentrations due to the availability of exchangeable sites.

Effect of pH: Fig. 5a-d shows the effect of pH in removing Ca^{2+} and Mg^{2+} from cooling tower water was studied by varying pH from 3 to 6. The results show that the highest % removal of Ca^{2+} was obtained at pH 3 from 25 to 98.58 using Amberlite IR120 and from 16.46 to 88.63 using Amberjet 1200. The highest % removal of Mg^{2+} was achieved from 20 to 98.33 using Amberlite IR1200 and from 21.67 to 86.92 % using Amberjet 1200 at pH 3. Higher adsorption was achieved at lower pH since heavy metals cations are completely adsorbed under more acidic conditions [15]. This could also be explained at lower pH values, the hydrogen ions compete with metal cation for the adsorption sites in the process, which result in releasing the later.

Adsorption isotherms: Adsorption isotherms are defined as the variation in the amount of gas adsorbed by the adsorbent with pressure at constant temperature can be expressed through a curve called adsorption isotherms. The most commonly used isotherms are Langmuir, Freundlich, Tempkin and D-R models. These mathematical models are mainly used and assumed that adsorption occurs when functional groups cover the surface

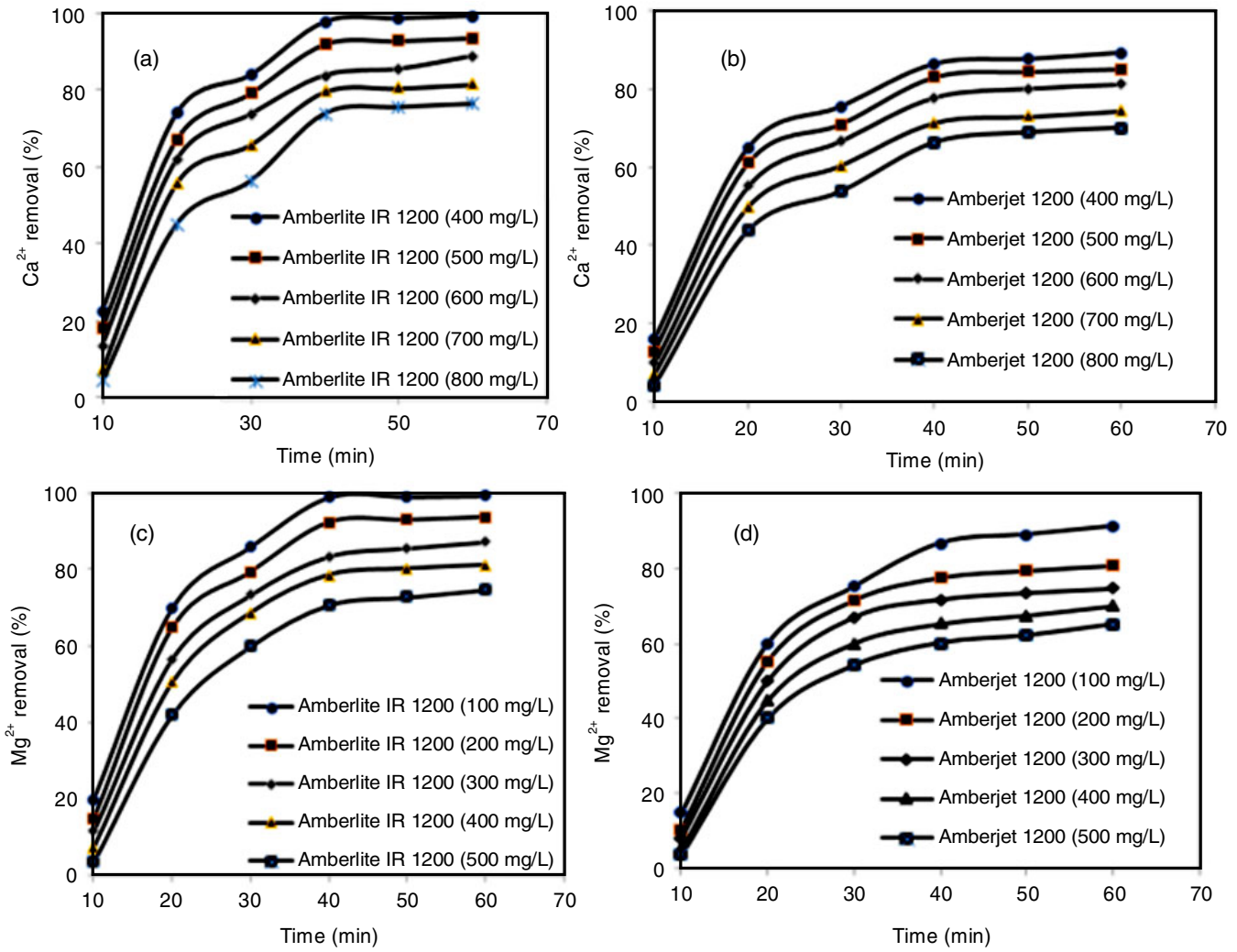

Fig. 4. Effect of concentration on the removal of Ca^{2+} and Mg^{2+} using Amberlite IR1200 (a and c) and Amberjet 1200 (b and d) (dosage = 15 mL, contact time = 60 min, pH = 3 and Temp. = 25 °C)

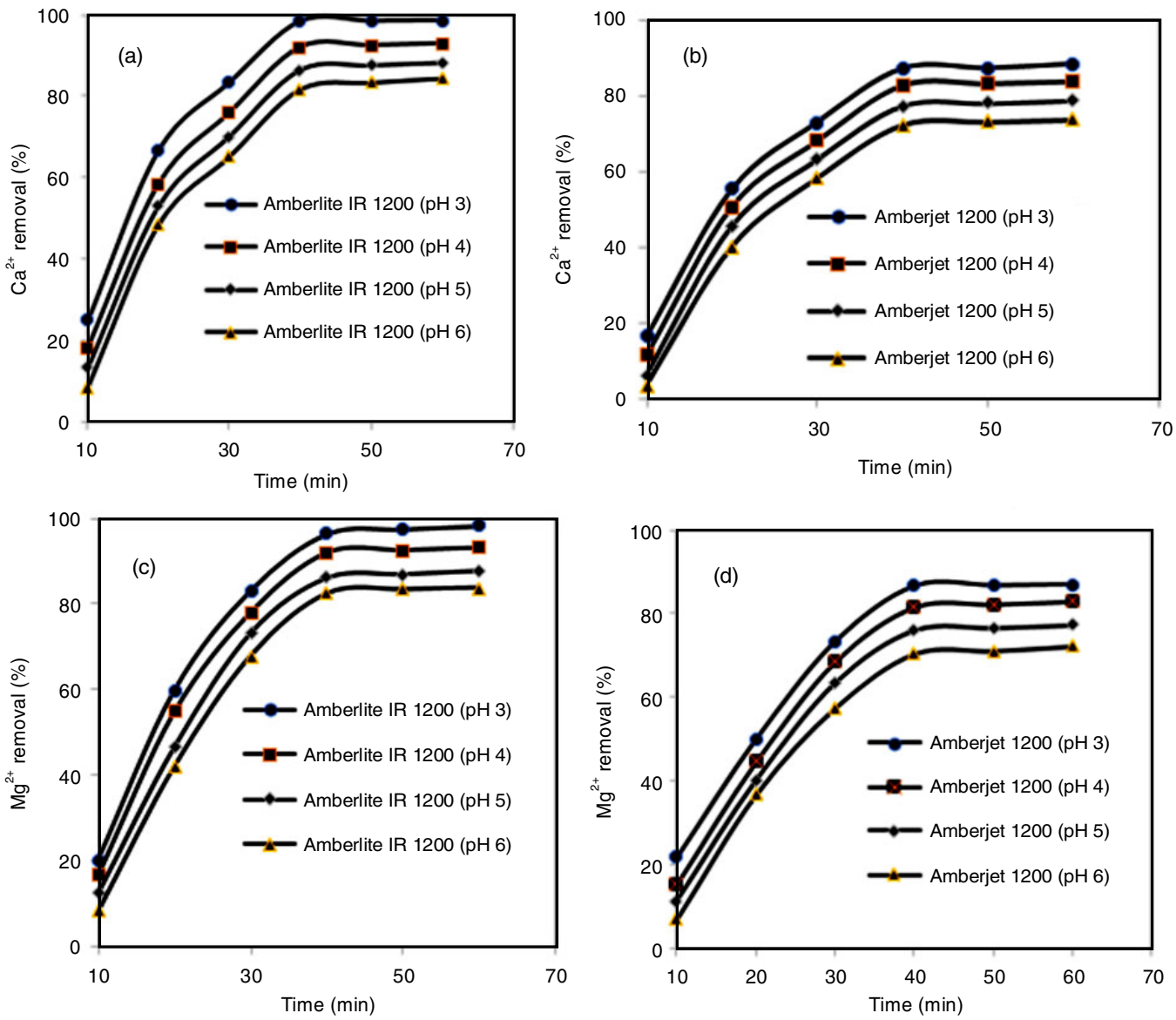

Fig. 5. Effect of pH on the removal of Ca^{2+} and Mg^{2+} using Amberlite IR1200 (a and c) and Amberjet 1200 (b and d) (Ca^{2+} = 600 ppm, Mg^{2+} = 300 ppm, contact time = 60 min, dosage = 15 mL and Temp. = 25 °C)

of the adsorbent. The metal uptake per unit weight of adsorbent to the equilibrium adsorbate concentrations in the fluid phase is related to these isotherms.

Langmuir isotherm model: The Langmuir model is based on the assumptions that each site can take one molecule and maximum adsorption occurs when a saturated monolayer of solute molecules is present on the adsorbent surface. The mathematical model of Langmuir is defined by eqn. 2:

$$q_e = \frac{q_m K_L C_e}{1 + K_L C_e} \quad (2)$$

where q_e is adsorbent equilibrium concentration (mg/g); q_m is the adsorbent capacity for monolayer adsorption (mg/g); K_L is equilibrium constant and C_e is the equilibrium concentration in the liquid phase (mg/L). Langmuir constants were determined by plotting ($1/q_e$) against ($1/C_e$) and rearranging eqn. 2 to form eqn. 3:

$$\frac{1}{q_e} = \frac{1}{q_m} + \frac{1}{q_m K_L}\frac{1}{C_e} \quad (3)$$

Several initial concentrations (400, 500, 600, 700 and 800 mg/L for Ca^{2+} and 100, 200, 300 and 400 mg/L for Mg^{2+}) were used at 298 K to obtain the results (Fig. 6). Amberlite IR1200 and Amberjet 1200 resins were plotted onto the same graph for comparative purposes. The correlation coefficients (r^2) were found to be 0.99493 (Amberlite IR120) and 0.99837 (Amberjet 1200) for Ca^{2+}, whereas Mg^{2+} correlation coefficients (R^2) were 0.97459 for Amberlite IR120 and 0.9574 for Amberjet 1200 as shown in Table-2. These correlation coefficients (R^2) indicates that equilibrium data fitted well Langmuir on both resins. Maximum adsorption capacities (Q_m) for Ca^{2+} were found to be 4, 2651 (b = 0, 1248) using Amberlite IR 120 and 4, 38 (b = 0.02732) using Amberjet 1200. Maximum adsorption capacity (Q_m) for Mg^{2+} were 2,688 (b = 0, 08932) using Amberlite IR120 and 2.7064 (b = 0.02182) using Amberjet 1200.

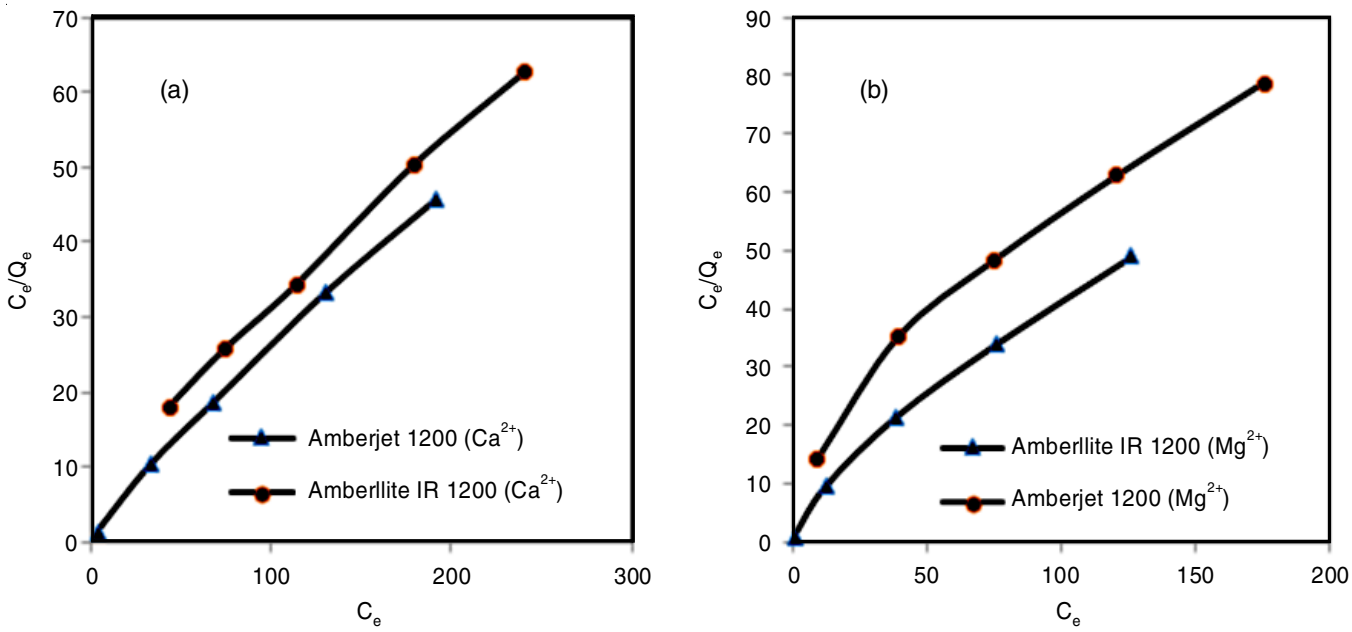

Fig. 6. Langmuir isotherm of Amberlite IR1200 (a) and Amberjet 1200 (b)

TABLE-2
ISOTHERMIC PARAMETERS OF Ca^{2+} AND Mg^{2+} REMOVAL ON AMBERLITE IR120 AND AMBERJET 1200

Isotherms	Amberlite IR120		Amberjet 1200	
	600 ppm	300 ppm	600 ppm	300 ppm
	Ca^{2+}	Mg^{2+}	Ca^{2+}	Mg^{2+}
Langmuir				
Q_m (mg/g)	4,265	2.688	4.380	2.706
R_L	0.125	0.089	0.027	0.0212
R^2	0.995	0.975	0.998	0.957
Freundlich				
K_f	2.312	0.735	0.932	0.237
1/n	0.108	0.251	0.261	0.434
R^2	0.958	0.990	0.973	0.997
Tempkin				
K_T (L/mg)	382.76	1.99	0.486	0.288
b_T	6738.59	7072.355	3011.31	4559.50
R^2	0.929	0.905	0.988	0.939
D-R model				
Q_m	1.771	1.912	1.753	1.689
E	0.88	0.62	10.9	5.46
R^2	0.571	0.684	0.879	0.695

Freundlich isotherm model: Freundlich isotherm model is an empirical equation based on adsorption on a heterogeneous surface defined by eqn. 4:

$$q_e = K_f C_e^{1/n} \quad (4)$$

The logarithm form of eqn. 4 forms eqn. 5:

$$\log q_e = \log K_f + \frac{1}{n}\log C_e \quad (5)$$

where K_f and n are the Freundlich constants, which represent the adsorption capacity and intensity.

Fig. 7a-b show the results of Freundlich isotherms obtained by plotting log Q_e *versus* log C_e. The results of Ca^{2+} removal show that correlation coefficients (r^2) were found to be 0.9579 for Amberlite IR120 and 0.9335 for Amberjet 1200. The results of Mg^{2+} removal indicates that the correlation coefficients were 0.99032 For Amberlite IR 1200 and 0.99651 for Amberjet 1200 indicating that the equilibrium data fitted well on both resins. The values of K_f and 1/n for Ca^{2+} removal was found to be 0.1078 and 0.2611 for Amberlite IR 120 and Amberjet 1200 and the K_f and 1/n values for Mg^{2+} removal were 0.2511 and 0.4337 for Amberlite IR120 and Amberjet 1200. The 1/n were between 0 and 1, meaning that both resins' adsorption of Ca^{2+} and Mg^{2+} were favourable at studied conditions.

Tempkin isotherm: Tempkin isotherm model considers the impact of indirect adsorbate/adsorbate interactions on the adsorption process; the adsorption heat of all molecules in the layer is also expected to decrease linearly due to the surface coverage. The Tempkin isotherm is only valid for intermediate ion concentrations [16]. By disregarding the incredibly low and high concentrations, the model assumes that heat of adsorption (function of temperature) of all particles in the layer would diminish straight instead of logarithmic with coverage [16]. The model is given by eqns. 6 and 7:

$$q_e = B \ln A_T + B \ln C_e \quad (6)$$

$$B = \frac{RT}{b_T} \quad (7)$$

where b_T = Temkin isorthem constant, A_T = Temkin isotherm equilibrium binding constant (L/g), R = universal gas constant (8.314 J/mol/K), T = temperature 298 K and B = constant related to heat of sorption (J/mol).

The binding constant of equilibrium (A_T) was found to be 382.76, 0.4859, 1.9929 and 0.2877 L g^{-1} indicate the maximum bonding energy and the adsorption heat constant b_T were found to be 6738.59, 3011.31, 7072.26 and 4559.50 KJ/mol. These constants are determined from the plot Q_e *versus* ln C_e and the values are shown in Table-2. Correlation coefficients (r^2) were found to be 0.93, 0.99, 0.90 and 0.94; it is concluded that this model fits well with the equilibrium data.

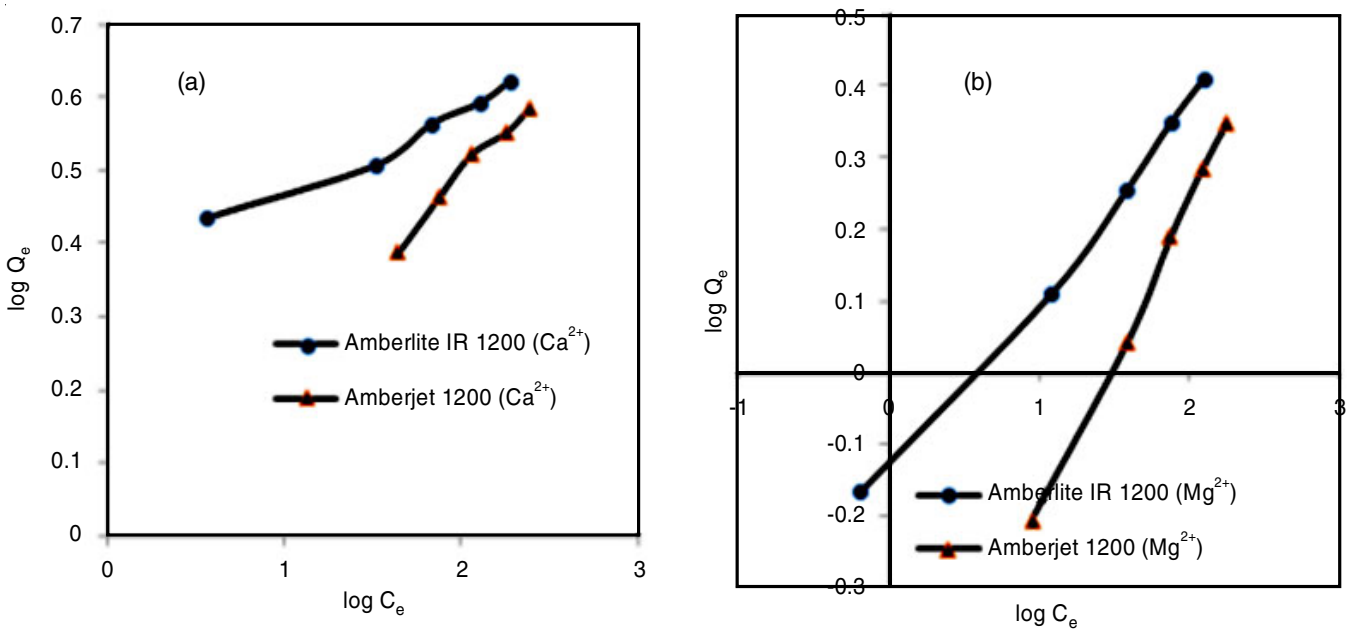

Fig. 7. Freundlich isotherm of Amberlite IR1200 (a) and Amberjet 1200 (b)

D-R model: The equilibrium data was applied to the D-R model to determine if adsorption occurred by the physical or chemical process. The adsorption potential is independent of the temperature, but it varies depending on the nature of adsorbent and adsorbate. The mean free energy of adsorption E gives information about adsorption mechanism as chemical ion exchange or physical adsorption.

The linearized form of the D-R isotherm is shown in eqn. 8:

$$\ln q_e = \ln q_m - \beta\varepsilon^2 \quad (8)$$

where β is the activity coefficient, which is related to mean adsorption energy (mol^2/J^2) and ε is the polanyi potential $\left[\varepsilon = RT\ln\left(1+\frac{1}{C_e}\right)\right]$. The mean adsorption energy, E (KJ/mol), is shown in eqn. 9:

$$E = \frac{1}{\sqrt{-2\beta}} \quad (9)$$

If E values are between 8 and 16 kJ/mol, the adsorption process follows by chemical ion exchange and if E is less than 8 kJ/mol, the adsorption is physical [17]. The mean adsorption energies (E) for removal of Ca^{2+} and Mg^{2+} using Amberlite and Amberjet were calculated as 0.88 kJ/mol for Ca^{2+} (Amberlite 1200), 10.45 KJ/mol for Ca^{2+} (Amberlite), 0.62 kJ/mol for Mg^{2+} (Amberlite) and 5.46 kJ/mol for Mg^{2+} (Amberjet 1200). These results indicate that the adsorption processes of metal ions were carried out *via* physical and chemical ion-exchange mechanisms (Table-3). Correlation coefficients (r^2) were found to be 0.57, 0.88, 0.68 and 0.69 (Table-2); it is concluded that this model does not fit well with the equilibrium data as compared to the Langmuir, Freundlich and Tempkin isotherm models.

The D-R model demonstrates if adsorption occurs by physical or chemical processes [18]. The linearized form of the D-R isotherm is shown in eqn. 10:

$$\ln q_e = \ln q_m - \beta\varepsilon^2 \quad (10)$$

where β is the activity coefficient, which is related to mean adsorption energy (mol^2/J^2) and ε is the polanyi potential $\left[\varepsilon = RT\ln\left(1+\frac{1}{C_e}\right)\right]$.

The mean adsorption energy [E (KJ/mol)] is shown in eqn. 11:

$$E = \frac{1}{\sqrt{-2\beta}} \quad (11)$$

TABLE-3
THERMODYNAMIC PARAMETERS FOR THE ADSORPTION OF Ca^{2+} AND Mg^{2+} ONTO AMBERLITE IR120 AND AMBERJET 1200 AT DIFFERENT TEMPERATURES

	K_d				ΔG°				ΔH°	ΔS°
	293 K	313 K	333 K	358 K	298 K	313 K	333 K	358 K		
Amberlite IR120										
Ca^{2+} (600 ppm)	0.044	0.061	0.1	0.557	8.34	6.68	5.02	2.94	32.69	0.083
Mg^{2+} (300 ppm)	0.044	0.057	0.111	0.475	8.33	6.75	5.16	3.17	31.62	0.080
Amberjet 1200										
Ca^{2+} (600 ppm)	0.024	0.032	0.043	0.066	9.18	8.89	8.59	8.29	13.47	0.0150
Mg^{2+} (300 ppm)	0.022	0.029	0.033	0.055	9.39	9.23	9.08	8.88	11.66	0.0078

Adsorption thermodynamics: The expected changes in the reaction should be considered when designing adsorption columns and monitoring how fast reactions (rate of reaction) occur. Knowing thermodynamic parameters is also essential in finding the expected change during the process. Ho [19] stated that the energy cannot be gained or lost in an isolated system to the surroundings, but enthalpy change is the driving force. The thermodynamic parameters (ΔH^o, ΔS^o and ΔG^o) for Ca^{2+} and Mg^{2+} adsorption onto resins were determined from the temperature-dependent adsorption. The estimations of enthalpy (ΔH^o) and entropy (ΔS^o) were determined from the slope and *y*-intercepts of the plot of ln K_d *versus* 1/T using applying eqns. 12 and 13:

$$K_d = \frac{C_o - C_e}{C_e}\frac{V}{m} \quad (12)$$

$$\ln K_d = \frac{\Delta S^o}{R} - \frac{\Delta H^o}{RT} \quad (13)$$

where C_o is the initial concentration (mg/L), C_e = equilibration concentration after centrifugation (mg/L), V = volume (mL), m = mass of millet husk (g), R (8.314 J mol^{-1} K^{-1}) is the ideal gas constant and T (K) is the temperature in Kelvin.

Free energy changes (ΔG^o) of specific adsorption are determined from eqn. 14:

$$\Delta G^\circ = \Delta H^\circ - T\Delta S^\circ \quad (14)$$

The values of ΔH^o in Table-3 for both Amberlite IR120 and Amberjet 1200 were between 1 to 93 kJ/mol demonstrating the physisorption. The positive estimations of ΔH^o demonstrate the endothermic type of adsorption, which suggests the chances of physical adsorption. In physical adsorption, while temperature increases, the degree of metal adsorption increases and there are no chances of chemisorption. Positive estimations of ΔG^o were obtained for both Amberlite IR1200 and Amberjet 1200 (Table-3) demonstrated that the ion exchange process is unfavourable and non-spontaneous. The positive estimations of ΔS^o demonstrated the increase temperatures were ascribed to the growth of pore size and activation of the adsorbent surface [4].

Kinetics studies: Lagergren's pseudo-first-order, pseudo-second-order and intraparticle diffusion models were used to clarify the adsorption kinetics of Ca^{2+} and Mg^{2+} removal from cooling tower water using Amberlite IR1200 and Amberjet 1200.

The Pseudo-first-order model is used to predict the rate of controlling mechanism based on adsorption capacity. Adsorption kinetics of Lagergren's pseudo-first-order is given by eqns. 15 and 16:

$$\frac{d_q}{e_t} = k_1(q_e - q) \text{ (Non-linear)} \quad (15)$$

$$\log(q_e - q) = \log q_e - \frac{k_1}{2.303}t \text{ (Linear)} \quad (16)$$

where q_e = amount of heavy metals adsorbed on the adsorbent at equilibrium (mg/g), q = amount of heavy metals adsorbed on the adsorbent at a particular time (mg/g) and K_1 = Pseudo first-order rate constant (min^{-1}).

The pseudo-second-order model for the adsorption of heavy metals onto the surface of adsorbents is applied when the obtained q_e is different from the derived one experimentally [20]. The non-linear (eqn. 17) and linear (eqn. 18) functions of pseudo-second-order are given below:

$$\frac{d_q}{d_t} = k_2(q_e - q)^2 \text{ (Non-linear)} \quad (17)$$

Integrating function (13) when t = 0 to t = t and q = 0 to q_e = q gives function (4.14)

$$\frac{1}{q_t} = \frac{1}{k_2(q_e)^2} + \frac{1}{q_e}t \text{ (Linear)} \quad (18)$$

where q_e = amount of heavy metals adsorbed on the adsorbent at equilibrium (mg/g), q = amount of heavy metals adsorbed on the adsorbent at a particular time (mg/g), K_2 = pseudo second-order rate constant (mg/g min), rate of reaction (k_2) is determined from the gradient of the linear graph of log (q_e-q) against time (t).

The concept of intraparticle diffusion is based on the Weber and Morris principle [21]. The model for intraparticular diffusion is stated in eqn. 19:

$$q_t = KIt^{0.5} + C \quad (19)$$

where KI is the constant of the intraparticle diffusion rate (g/mg/$min^{0.5}$), q_t is the adsorption capacity (mg/g) at time t (min) and C is a constant that indicates the thickness boundary layer, the higher the value of C, the more significant the impact of the boundary layer.

The rate of reaction (k_1) is determined from the gradient of the linear graph of log (q_e-q) against time (t). The plot of ln (Q_e-Q_t) against t is shown in Fig. 8a. The linear plots of pseudo-second-order and intraparticle models are shown in Fig. 8b-c, respectively. The R^2 values of pseudo-first-order, pseudo-second-order and intraparticle models ranged from 0.89 to 1 on both metals (Table-4). This observation indicates that pseudo-first-order, pseudo-second-order and intraparticle diffusion models best describe the experimental data in removing Ca^{2+} and Mg^{2+} from cooling tower water. The rate constants k_1 and k_2, correlation of coefficients of the plots together with Q_e values are given in Table-4.

Conclusion

This study aimed at thermodynamic and kinetic studies in removing Ca^{2+} and Mg^{2+} ions from cooling tower water using Amberlite IR120 and Amberjet 1200. The highest % removal of Ca^{2+} was found to be 99.59% using Amberlite IR1200 and 91.33% using Amberjet 1200 at the resins dosage of 35 mL. Another highest adsorption % removal in the removal was 99.33 % using Amberlite and 91.17% using Amberjet at the resins dosage of 35 mL. The correlation coefficients (R^2) of Langmuir, Freundlich and Tempkin isotherms were found to range from 0.92 to 1, which suggests that experimental data best described the models. However, correlation coefficients (R^2) for the D-R model range between 0.5 to 0.8, meaning that experimental data does not fit the model. The values of ΔH^o for both Amberlite IR120 and Amberjet 1200 were between 1 to 93 kJ/mol demonstrating the physisorption. The positive

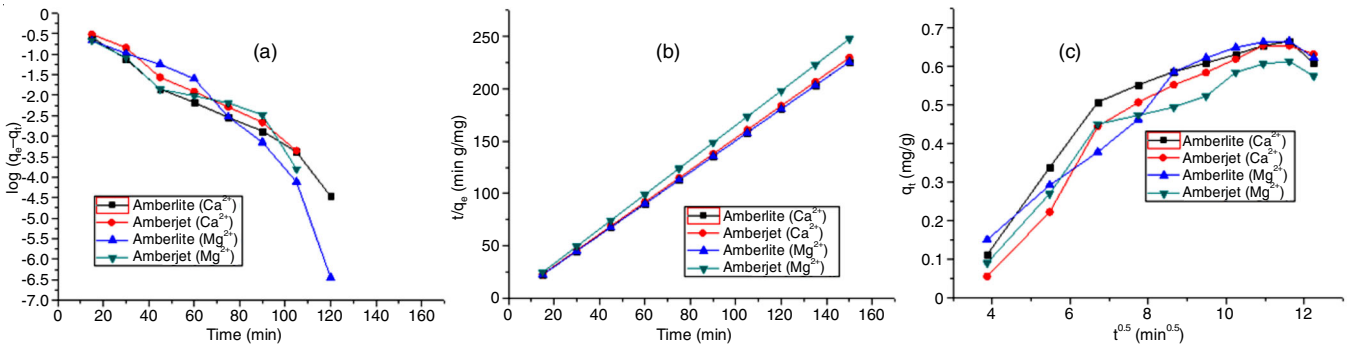

Fig. 8. Pseudo-first-order (a), pseudo-second-order (b) and intraparticle diffusion models (c)

TABLE-4
KINETICS PARAMETERS FOR ION EXCHANGE OF Ca^{2+} AND Mg^{2+} FROM COOLING TOWER WATER

Kinetics	Amberlite IR120		Amberjet 1200	
	600 ppm	300 ppm	600 ppm	300 ppm
	Ca^{2+}	Mg^{2+}	Ca^{2+}	Mg^{2+}
Pseudo-first order				
K_1	0.0767	0.0767	0.0767	0.0767
R^2	0.972	0.989	0.972	0.989
Pseudo-second order				
K_2	0	0	0	0
R^2	1	1	1	1
Intraparticle diffusion				
K_i (mg/g $min^{1/2}$)	0.0651	0.0763	0.0626	0.0565
C	0.02	0.16	0.34	0.24
R^2	0.864	0.911	0.903	0.861

value of ΔHº demonstrated the endothermic type of adsorption, which suggests the chances of physical adsorption. In physical adsorption, while temperature increases, the degree of metal adsorption increases and no chances of chemisorption process. Positive values of ΔGº for both Amberlite IR1200 and Amberjet 1200 demonstrated that the ion exchange process is unfavourable and non-spontaneous. The R^2 values of pseudo-first-order, pseudo-second-order and intraparticle models ranged from 0.89 to 1 on both metal ions. This observation indicates that pseudo-first-order, pseudo-second-order and intraparticle diffusion models describe the best experimental data for the removal of Ca^{2+} and Mg^{2+} ions from cooling tower water.

CONFLICT OF INTEREST

The authors declare that there is no conflict of interests regarding the publication of this article.

REFERENCES

1. D.E. Abd-El-Khalek, B.A. Abd-El-Nabey, M.A. Abdel-kawi, S.R. Ramadan and I. Desalin, *Water Treat.*, **57**, 2870 (2016); https://doi.org/10.1080/19443994.2014.987174
2. D.M. Dronov, A.V. Gontovoy, Y.N. Sarkisyan and N.V. Karandeeva, *Nucl. Energy Technol.*, **7**, 85 (2021); https://doi.org/10.3897/nucet.7.68940
3. L. Gurreri, A. Tamburini, A. Cipollina and G. Micale, *Membranes*, **10**, 146 (2020); https://doi.org/10.3390/membranes10070146
4. A.A. Adeyi, T.G. Abayomi, M.K. Purkait and P. Mondal, *Open J. Appl. Sci.*, **9**, 544 (2019); https://doi.org/10.4236/ojapps.2019.97043
5. S. Indika, Y. Wei, D. Hu, J. Ketharani, T. Ritigala, T. Cooray, M.A.C.K. Hansima, M. Makehelwala, K.B.S.N. Jinadasa, S.K. Weragoda and R. Weerasooriya, *Membranes*, **11**, 383 (2021); https://doi.org/10.3390/membranes11060383
6. D. Ouyang, Y. Zhuo, L. Hu, Q. Zeng, Y. Hu and Z. He, *Minerals*, **9**, 291 (2019); https://doi.org/10.3390/min9050291
7. M.T. Bankole, A.S. Abdulkareem, I.A. Mohammed, S.S. Ochigbo, J.O. Tijani, O.K. Abubakre and W.D. Roos, *Sci. Rep.*, **9**, 4475 (2019); https://doi.org/10.1038/s41598-018-37899-4
8. Z. Zhang, T. Wang, H. Zhang, Y. Liu and B. Xing, *Sci. Total Environ.*, **757**, 143910 (2021); https://doi.org/10.1016/j.scitotenv.2020.143910
9. M. Mojziš, T. Bubeníková, M. Zachar, D. Kaèíková and J. Štefková, *BioResources*, **14**, 8738 (2019); https://doi.org/10.15376/biores.14.4.8738-8752
10. M. Banza and H. Rutto, *J. Environ. Sci. Heal. Part A*, **57**, 117 (2022); https://doi.org/10.1080/10934529.2022.2036552
11. M. Korkmaz, C. Özmetin, B. Fil and Y. Yasar, *Igdir Univ. J. Inst. Sci. Technol.*, **3**, 47 (2012); https://hdl.handle.net/20.500.12462/4370
12. F. Morante-Carballo, N. Montalván-Burbano, P. Carrión-Mero and N. Espinoza-Santos, *Sustainability*, **13**, 7751 (2021); https://doi.org/10.3390/su13147751
13. A. Agrawal and K.K. Sahu, *J. Hazard. Mater.*, **B137**, 915 (2006); https://doi.org/10.1016/j.jhazmat.2006.03.039
14. A. Addala, M. Boudiaf, M. Elektorowicz, E. Bentouhami and Y. Bengeurba, *Water Sci. Technol.*, **84**, 1206 (2021); https://doi.org/10.2166/wst.2021.309
15. O.O. Sadare, A.O. Ayeni and M.O. Daramola, *Chem. Eng. Trans.*, **80**, 361 (2020); https://doi.org/10.3303/CET2080061
16. G. Purwiandono, P. Lestari, W. Widodo, M. Marlina and N. Aprilia, *J. Chem. Res.*, **3**, 47 (2018); https://doi.org/10.20885/ijcr.vol2.iss1.art6
17. F. Helfferich, *J. Phys. Chem.*, **66**, 39 (1962); https://doi.org/10.1021/j100807a008
18. J. Kabuba and M. Banza, *Results Eng.*, **8**, 100189 (2020); https://doi.org/10.1016/j.rineng.2020.100189
19. Y.S. Ho, *Water Res.*, **37**, 2323 (2003); https://doi.org/10.1016/S0043-1354(03)00002-2
20. Y. Ho and G. McKay, *Trans. IChemE*, **76**, 183 (1998).
21. W.J. Weber and J.C. Morris, *J. Sanit. Eng. Div.*, **89**, 31 (1963); https://doi.org/10.1061/JSEDAI.0000430